Open-Framework Structures

DOI: 10.1002/ange.200502413

A Building-Up Process in Open-Framework Metal Carboxylates that Involves a Progressive Increase in Dimensionality**

*Meenakshi Dan and C. N. R. Rao**

Dedicated to Professor Herbert W. Roesky on the occasion of his 70th birthday

Extensive research work has been carried out in the last few years on the synthesis and characterization of several families of open-framework materials, including aluminosilicates,[1] phosphates,[2] and carboxylates.[3] These studies have shown the occurrence of a variety of three-dimensional (3D) architectures containing channels and other features. A crucial problem with these materials relates to the mechanism of formation, an aspect that assumes special significance because these materials are generally synthesized under

[*] M. Dan, Prof. Dr. C. N. R. Rao
Chemistry and Physics of Materials Unit and
CSIR Centre of Excellence in Chemistry
Jawaharlal Nehru Centre for Advanced Scientific Research
Jakkur P. O., 560064 Bangalore (India)
and
Solid State and Structural Chemistry Unit
Indian Institute of Science
560012 Bangalore (India)
Fax: (+91) 80-2208-2766
E-mail: cnrrao@jncasr.ac.in

[**] M.D. thanks the CSIR (India) for a Senior Research Fellowship.

hydro- or solvothermal conditions. An important suggestion in this context is the role of the secondary building units (SBUs) in the building-up of the 3D structures.[4] Recent studies of open-framework metal phosphates have shown how low-dimensional structures transform into higher-dimensional ones under mild conditions.[5] Thus, a zero-dimensional zinc phosphate comprising a four-membered ring has been shown to transform into a 3D sodalite-related structure, thereby providing an example of a molecule-to-material transformation.[6] While these studies are of significance, the question regarding the mode of formation of these structures still remains, since a given set of polyhedra can, in principle, generate a variety of three-dimensional structures through different rearrangements.[7] We therefore considered it important to investigate the process of formation of three-dimensional, open-framework structures that do not contain polyhedral anions, and chose to study the transformations of metal carboxylates.

We started with the zero-dimensional molecular zinc oxalate, $(C_4N_2H_{12})_3[Zn_2(C_2O_4)_5]\cdot 8H_2O$ (**1**), which has the dimeric structure shown in Figure 1a. On heating **1** in the presence of piperazine (PIP) at 100 °C for 48 h, we obtained a compound of the formula $(C_4N_2H_{12})_2[Zn_2(C_2O_4)_4]\cdot 3H_2O$ (**2**). Heating **1** at 165 °C in the presence of PIP for 48 h gave $(C_4N_2H_{12})_3[Zn_4(C_2O_4)_7]\cdot 4H_2O$ (**3**), whereas heating **1** at 180 °C for the same time period gave $(C_4N_2H_{12})[Zn_2(C_2O_4)_3]$ (**4**). We illustrate these transformations by showing the powder XRD patterns of the products recorded at different temperatures (Figure 2). Significantly, we did not find the presence of any other compounds during the transformations, as evidenced from the powder XRD patterns recorded periodically as the transformation progressed. A crystallographic study of **2**–**4** indicated that **2** has a linear-chain structure (Figure 1b), while **3** has a structure with honeycomb apertures (Figure 1c). Compound **4** is three-dimensional with a network of interconnected channels (Figure 3). Thus, as the reaction temperature is increased, the overall dimensionality of the product increases. Furthermore, the water content decreases as we go from **1** to **4**, and this is accompanied by an increase in the relative proportion of Zn with respect to the oxalate or the amine.

A brief description of the structures of **2**–**4** is in order. In the one-dimensional helical chain structure of **2**, each zinc atom is surrounded by six oxygen atoms from three oxalate units. There are two types of oxalate units, one of which binds to a Zn atom and has two terminal O atoms, and another which is a bis-chelating, bridging oxalate unit that binds to two Zn atoms. The one-dimensional helical chains run parallel to the *c*-axis of the unit cell (Figure 1b). The transformation product of the dimer at 165 °C, **3**, has a double-stranded 1D structure and contains two types of oxalate units just as in **2**. The two Zn atoms in the asymmetric unit are in different coordination environments: one is surrounded by six O atoms of the two bridging and one hanging oxalate molecules, whereas the other is surrounded by six O atoms of three bridging oxalate units. This results in condensation of the single-stranded, one-dimensional zinc oxalate chains to form a pseudo-two-dimensional zinc oxalate structure, with a honeycomb aperture, parallel to the *bc*-plane

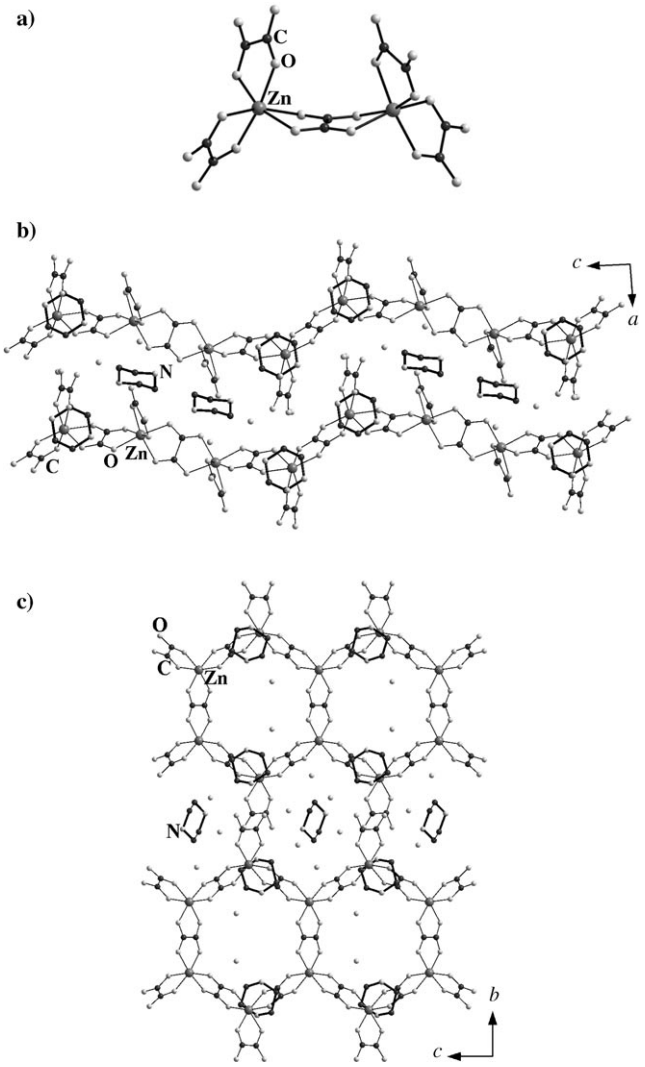

Figure 1. a) Structure of the zero-dimensional zinc oxalate dimer **1**. b) The helical chains in **2** viewed down the *b*-axis of the unit cell. Amine and interstitial water molecules are also shown. c) The pseudo-two-dimensional zinc oxalate **3** viewed down the *a*-axis of the unit cell. Note the honeycomb apertures.

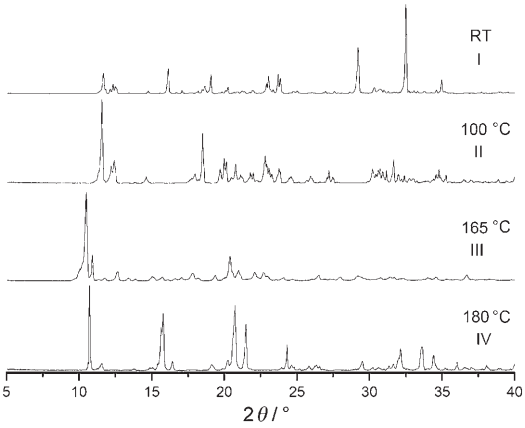

Figure 2. Powder XRD patterns of the products obtained by heating **1** at different temperatures for 48 h in the presence of piperazine.

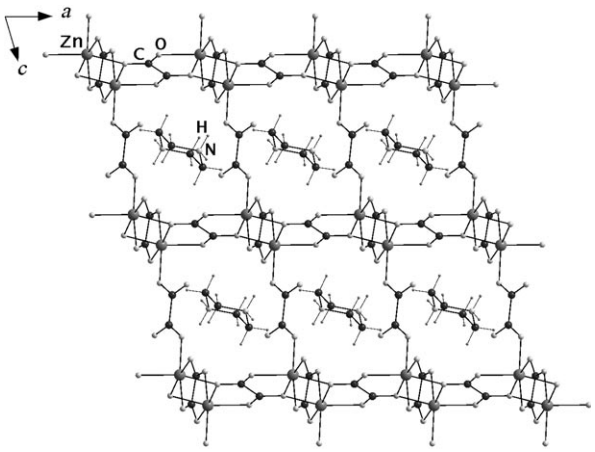

Figure 3. The three-dimensional structure of **4** formed by the pillaring of the layers by bridging oxalate groups. Protonated piperazine molecules are located in cages formed by the intersection of the channels running along the three crystallographic directions of the unit cell.

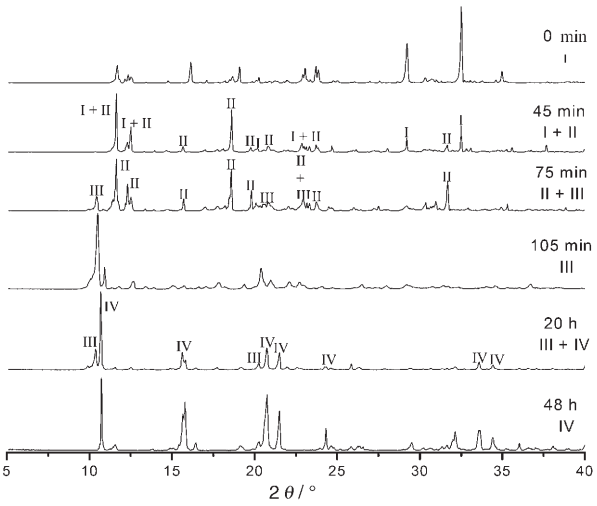

Figure 4. Changes of **1** during heating at 180 °C. Powder XRD patterns show the evolution of different phases with increasing dimensionality as a function of time.

of the unit cell (Figure 1 c). There are three types of oxalates in the three-dimensional structure of **4**: one bis-chelating and bridging oxalate moiety binding to two Zn atoms, a monodentate bridging oxalate which binds two Zn atoms and has two terminal O atoms, and another bis-chelating and triply bridging oxalate unit with three coordinated O atoms that binds four Zn atoms. The Zn atoms are connected by bridging oxalate units and three-coordinate O atoms to form layers parallel to the *ab*-plane of the unit cell. These layers are cross-linked by bridging oxalate units to form a three-dimensional architecture with a network of interconnected channels running along all the three crystallographic directions of the unit cell (Figure 3).

In order to understand the formation of the higher-dimensional oxalates from zero-dimensional **1** the progress of the conversion was monitored after different reaction times. On heating **1** at 100 °C with PIP for 9 h, the chain structure **2** appears, its proportion increasing progressively with time. After 48 h, **1** has been entirely transformed into **2**. When the reaction is carried out at 165 °C, formation of **2** is observed within 4 h, with the transformation to **2** being complete in 16 h. After 20 h, we noticed the appearance of **3**, accompanied by a decrease in the proportion of **2**. After 48 h, we obtained **3** as the sole product. When the study was carried out at 180 °C, we obtained all the three structures progressively, as shown by the powder XRD patterns in Figure 4. Thus, within 45 min, **1** starts transforming into **2** and as this transformation nears completion **2** starts transforming into **3**, as can be seen after 75 min of the reaction when a mixture of both **2** and **3** is present. After 105 min of the reaction **2** has been completely transformed into **3**, which then starts to transform into **4**. Thus, after 20 h of the reaction both **3** and **4** are present. After about 48 h, **3** has been transformed entirely into **4**. This study demonstrates that the three-dimensional structure emerges from the building-up of the lower-dimensional structures. This transformation involves hydrolysis and condensation, wherein the oxalate moiety is eliminated to form the higher-dimensional structures, accompanied by dehydration (Figure 5). On increasing the reaction temperature, the dimensionality of the structure increases as the total water content decreases, and this is accompanied by an increase in the number of zinc atoms bonding to the oxalate units (Zn/oxalate ratio).

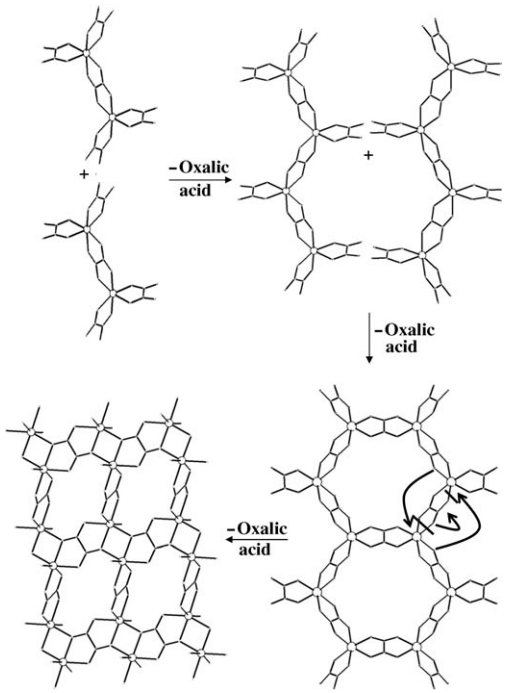

Figure 5. Formation of chain (**2**), pseudo-two-dimensional (**3**), and three-dimensional (**4**) structures from zero-dimensional **1** by hydrolysis/condensation.

We have also found that the nickel propionate dimer $[Ni(CH_3CH_2CO_2)_2(H_2O)]$ (**5**) transforms into a one-dimensional chain structure $[Ni(CH_3CH_2CO_2)_2]$ (**6**) at 25 °C within 24 h (Figure 6). The dimer has two Ni atoms connected by

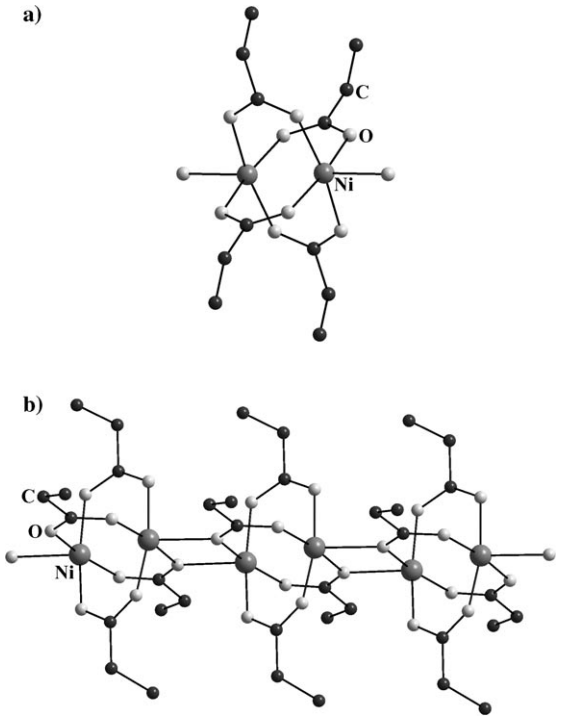

Figure 6. a) The nickel propionate dimer **5**. b) The nickel propionate chain **6**.

four bridging propionate groups in a paddlewheel-type architecture similar to that found in copper and other metal acetate dimers, as well as in many metal carboxylates.[8] The facile formation of the chain structure from the dimer can be visualized as a result of the self-assembly of the dimers followed by the elimination of water. The chain structure of **6** is formed by the joining of the dimer through the three-coordinate propionate oxygen atoms. Thus, there are two types of propionate units in **6**, one bridging the two Ni atoms and the other joining the dimers through the three-coordinate oxygen atoms as well as bridging the two Ni atoms to form chains running parallel to the *a*-axis. The metal-to-ligand ratio increases as the dimer transforms into the chain, with a concomitant decrease in the water content.

We found a similar building-up process in the cobalt succinates described by Férey and coworkers.[9] Accordingly, $[Co(H_2O)_4(C_4H_4O_4)]$, with a linear-chain structure, transforms into the layered complex $[Co_4(OH)_2(H_2O)_2(C_4H_4O_4)_3]\cdot 2H_2O$ on heating in water at 150 °C, as evidenced from XRD studies. It would therefore appear that the progressive formation of higher-dimensional structures of cobalt succinates with increasing temperature reported recently by Forster and Cheetham[10] occurs through such molecular transformations.

In the case of the transformation of **5** into **6**, we recognize that the aggregation of paddlewheel clusters is known,[11] but the transformation described by us has features comparable to those of the zinc oxalates. In conclusion, we feel that the low-D to high-D transformations discussed by us are likely to occur by a building-up process in solution, rather than by a decomposition or reformation process. The kinetic data lend some support to this observation. It is noteworthy that a 1,4-benzenedicarboxylate has recently been shown to undergo a 1D to 3D transformation.[12]

Experimental Section

The zinc oxalate dimer **1** was synthesized by the procedure described earlier.[13] The transformation reactions were carried out in a 7-mL, PTFE-lined acid digestion bomb. Heating of **1** (121.1 mg) with piperazine (10.8 mg; ratio **1**/PIP = 2:1) in H_2O (2 mL) at 100 °C, 165 °C, or 180 °C for 48 h yielded **2**, **3**, and **4**, respectively. The products were generally single-crystalline, although the starting zinc oxalate dimer was used in the form of a fine powder.

In a typical synthesis of nickel propionates **5** and **6**, NiO (1 g) was dispersed in propionic acid/water (4 mL, 1:1 (v/v)) and the mixture was heated in a 23-mL, PTFE-lined acid digestion bomb at 75 °C for 48 h. The reaction resulted in the formation of deep-green, rod-shaped crystals of **6**. The filtrate at room temperature gave green crystals **5**.

Single-crystal structure determination by X-ray diffraction was performed with a Siemens Smart-CCD diffractometer equipped with a normal focus, 2.4-kW, sealed-tube X-ray source ($Mo_{K\alpha}$ radiation, $\lambda = 0.71073$ Å) operating at 40 kV and 40 mA. The structure was solved by direct methods using SHELXS-86.[14] An empirical absorption correction based on symmetry-equivalent reflections was applied using the SADABS program.[15] All the hydrogen positions were initially located in the difference Fourier maps and the hydrogen atoms were placed geometrically and held in the riding mode for the final refinement. Full-matrix least-squares structure refinement against $|F^2|$ was carried out using the SHELXTL-PLUS package of programs.[16]

Crystal data: **2**: $C_{16}H_{30}N_4O_{19}Zn_2$, $M_r = 713.18$; monoclinic, space group $C2/c$, $a = 15.2706(3)$, $b = 9.0584(1)$, $c = 38.2638(1)$ Å, $\beta = 90.40°$; $V = 5292.8(1)$ Å^3; $Z = 8$; $\rho_{calcd} = 1.790$ g cm^{-3}, $T = 298$ K, $\mu = 1.907$ mm^{-1}; 10672 reflections measured with 3799 independent reflections; $R_{int} = 0.0399$; $R_1 = 0.0457$, $wR_2 = 0.1113$ (observed data) and $R_1 = 0.0633$, $wR_2 = 0.1233$ (all data). **3**: $C_{26}H_{44}N_6O_{32}Zn_4$, $M_r = 584.9$; monoclinic, space group $P2_1/m$, $a = 8.7924(9)$, $b = 35.595(4)$, $c = 9.2583(10)$ Å, $\beta = 96.602(2)°$; $V = 2878.3(5)$ Å^3; $Z = 4$. While the structure of the compound could be solved, the R values were large due to the rather poor quality of the crystals. **4**: $C_{10}H_{12}N_2O_{12}Zn_2$, $M_r = 241.48$; triclinic, space group $P\bar{1}$, $a = 5.8208(9)$, $b = 7.6266(11)$, $c = 8.5782(13)$ Å, $\alpha = 88.272(3)°$, $\beta = 73.81°$, $\gamma = 86.599(3)°$; $V = 365.02(9)$ Å^3; $Z = 2$; $\rho_{calcd} = 2.197$ g cm^{-3}, $T = 298$ K, $\mu = 3.362$ mm^{-1}; 1562 reflections measured with 1040 independent reflections; $R_{int} = 0.0291$; $R_1 = 0.0418$, $wR_2 = 0.0921$ (observed data) and $R_1 = 0.0577$, $wR_2 = 0.1006$ (all data). **5**: $C_6H_{12}NiO_5$, $M_r = 885.42$; monoclinic, space group $P2_1/c$, $a = 15.384(1)$, $b = 17.381(1)$, $c = 15.174(1)$ Å, $\beta = 94.407(1)°$; $V = 4045.4(3)$ Å^3; $Z = 4$; $\rho_{calcd} = 1.454$ g cm^{-3}, $T = 298$ K, $\mu = 1.902$ mm^{-1}; 16311 reflections measured with 5771 independent reflections; $R_{int} = 0.0808$; $R_1 = 0.0480$, $wR_2 = 0.1279$ (observed data) and $R_1 = 0.0557$, $wR_2 = 0.1404$ (all data). **6**: $C_6H_{10}NiO_4$, $M_r = 204.85$; triclinic, space group $P\bar{1}$, $a = 5.1954(2)$, $b = 8.4555(1)$, $c = 9.5431(4)$ Å, $\alpha = 91.720(2)$, $\beta = 91.789(2)$, $\gamma = 105.078(2)°$; $V = 404.28(2)$ Å^3; $Z = 2$; $\rho_{calcd} = 1.683$ g cm^{-3}, $T = 298$ K, $\mu = 2.362$ mm^{-1}; 1691 reflections measured with 1135 independent reflections; $R_{int} = 0.0202$; $R_1 = 0.0313$, $wR_2 = 0.0785$ (observed data) and $R_1 = 0.0377$, $wR_2 = 0.0820$ (all data).

CCDC-276975 (**2**), -277863 (**3**), -276977 (**4**), -276978 (**5**), and -276979 (**6**) contain the supplementary crystallographic data for this paper. These data can be obtained free of charge from The Cambridge Crystallographic Data Centre via www.ccdc.cam.ac.uk/data_request/cif.

Received: July 11, 2005
Revised: September 28, 2005
Published online: November 30, 2005

Keywords: carboxylate ligands · materials science · solid-state structures · supramolecular chemistry · zinc

[1] W. M. Meier, D. H. Oslen, C. Baerlocher, *Atlas of Zeolite Structure Types*, Elsevier, London, **1996**.
[2] A. K. Cheetham, G. Férey, T. Loiseau, *Angew. Chem.* **1999**, *111*, 3466; *Angew. Chem. Int. Ed.* **1999**, *38*, 3268.
[3] C. N. R. Rao, S. Natarajan, R. Vaidhyanathan, *Angew. Chem.* **2004**, *116*, 1490; *Angew. Chem. Int. Ed.* **2004**, *43*, 1466.
[4] G. Férey, *J. Solid State Chem.* **2000**, *152*, 37; G. Férey, C. Serre, C. Mellot-Draznieks, F. Millange, S. Surblé, J. Dutour, I. Margiolaki, *Angew. Chem.* **2004**, *116*, 6456; *Angew. Chem. Int. Ed.* **2004**, *43*, 6296; M. E. Eddaoudi, D. B. Moler, H. Li, B. Chen, T. M. Reineke, M. O'Keeffe, O. M. Yaghi, *Acc. Chem. Res.* **2001**, *34*, 319; M. E. Eddaoudi, J. Kim, D. Vodak, A. Sudik, J. Wachter, M. O'Keeffe, O. M. Yaghi, *Proc. Natl. Acad. Sci. USA* **2002**, *99*, 4900; O. M. Yaghi, M. O'Keeffe, N. W. Ockwig, H. K. Chae, M. Eddaoudi, J. Kim, *Nature* **2003**, *423*, 705.
[5] S. Oliver, A. Kuperman, G. A. Ozin, *Angew. Chem.* **1998**, *110*, 48; *Angew. Chem. Int. Ed.* **1998**, *37*, 46; C. N. R. Rao, S. Natarajan, A. Choudhury, S. Neeraj, A. A. Ayi, *Acc. Chem. Res.* **2003**, *36*, 80; A. Choudhury, S. Neeraj, S. Natarajan, C. N. R. Rao, *J. Mater. Chem.* **2001**, *11*, 1537; A. A. Ayi, A. Choudhury, S. Natarajan, S. Neeraj, C. N. R. Rao, *J. Mater. Chem.* **2001**, *11*, 1181; R. I. Walton, F. Millange, A. L. Bail, T. Loiseau, C. Serre, D. O'Hare, G. Férey, *Chem. Commun.* **2000**, 203; A. J. Norquist, D. O'Hare, *J. Am. Chem. Soc.* **2004**, *126*, 6673.
[6] M. Dan, D. Udayakumar, C. N. R. Rao, *Chem. Commun.* **2003**, 2212; R. Murugavel, M. G. Walawalkar, M. Dan, H. W. Roesky, C. N. R. Rao, *Acc. Chem. Res.* **2004**, *37*, 763.
[7] C. Mellot-Draznieks, J. Dutour, G. Férey, *Angew. Chem.* **2004**, *116*, 6450; *Angew. Chem. Int. Ed.* **2004**, *43*, 6290.
[8] M. E. Eddaoudi, J. Kim, J. B. Wachter, H. K. Chae, M. O'Keeffe, O. M. Yaghi, *J. Am. Chem. Soc.* **2001**, *123*, 4368; M. J. Rosseinsky, *Microporous Mesoporous Mater.* **2004**, *73*, 15.
[9] C. Livage, C. Egger, G. Férey, *Chem. Mater.* **2001**, *13*, 410.
[10] P. M. Forster, A. R. Burbank, C. Livage, G. Férey, A. K. Cheetham, *Chem. Commun.* **2004**, 368.
[11] F. A. Cotton, E. A. Hillard, C. A. Murillo, H.-C. Zhou, *J. Am. Chem. Soc.* **2000**, *122*, 416.
[12] A. Thirumurugan, C. N. R. Rao, *J. Mater. Chem.* **2005**, *15*, 3852.
[13] R. Vaidhyanathan, S. Natarajan, C. N. R. Rao, *J. Chem. Soc. Dalton Trans.* **2001**, 699.
[14] G. M. Sheldrick, *SHELXS-86 Program for Crystal Structure Determination*, University of Göttingen, Germany, **1986**; G. M. Sheldrick, *Acta Crystallogr. Sect. A* **1990**, *46*, 467.
[15] G. M. Sheldrick, *SADABS: Siemens Area Detector Absorption Correction program*, University of Göttingen, Germany, **1994**.
[16] G. M. Sheldrick, *SHELXS-93 Program for Crystal Structure Solution and Refinement*, University of Göttingen, Germany, **1993**.

